Progress In Electromagnetics Research C, Vol. 38, 177–190, 2013

DESIGN OF DIPLEXER WITH ROTATIONALLY SYMMETRIC STRUCTURE

Sai Wai Wong*, Xiao-Han Liu, Kai Wang, Ruisen Chen, Li-Sheng Zheng, and Qing-Xin Chu

School of Electronic and Information Engineering, South China University of Technology, Guangzhou, China

Abstract—This paper presents an approach to the design of novel diplexers with pairs of transmission zeros for each output port. A rotationally symmetric structure with shorted circuited stubs is proposed to achieve diplexer operation, and the diplexer exhibits a good filtering performance with a pair of transmission zeros allocated at two sides of the passbands as well. The analysis of the rotationally symmetric structure bandpass filter is also presented in this paper in detail. Moreover, the interdigital coupled-lines are introduced to improve the out-of-band performance of the proposed rotationally symmetric diplexer. In order to verify the proposed structure, first a diplexer with rotationally structure operating at 2.4/2.73 GHz with simulated insertion loss of 1.217/0.930 dB is designed and simulated, then a diplexer with interdigital coupled-lines operating at 5/5.8 GHz with measured insertion loss of 1.524/1.524 dB is designed, simulated and measured to improve the passband selectivity, and the measured results are in good agreement with simulated ones.

1. INTRODUCTION

Recent rapid developments in modern wireless communication industry have required the radio frequency (RF) components to operate at multiple frequency bands. Many efforts have been made to develop more versatile passband components such as antennas [1–4], filters [5–8] and transformers [9, 10]. Meanwhile, the diplexer as one of the most important passive circuits has been widely used in microwave and communication systems. The most popular structures to form the planar diplexer are combing two bandpass filters with different

Received 27 February 2013, Accepted 20 March 2013, Scheduled 28 March 2013

* Corresponding author: Sai Wai Wong (eewsw@scut.edu.cn).

frequencies and two matching circuits [10, 11]. However, this idea may increase insertion loss and circuit size [12, 13]. A novel structure with compact size using microstrip-line technology is introduced in [14]. On the other hand, a good band isolation is another important target for designing diplexer. By using the stepped impedance resonator (SIR) and a good impedance matching at input port for two BPFs, a high isolation between two passbands is obtained in [15, 16]. In [17], a microstrip-line resonator with loaded elements is proposed and studied to design a microstrip diplexer. Different loads on different positions of the resonator make it exhibit different features, and it can be used to control the characteristics of the diplexer.

In this paper, a diplexer based on rotationally symmetric structure is proposed. Firstly, the circuit model of rotationally symmetric structure is analyzed [18], and then the model of the rotational structure with coupling effect is considered and analyzed. A pair of transmission zeros is generated near the lower and upper cut-off frequencies by means of analysis. To make use of this outstanding characteristic of rotationally structure, a diplexer is designed at 2.4/2.73 GHz and exhibits a good filtering performance. Moreover, the interdigital coupled-line is introduced to improve the passband selectivity. Another diplexer with interdigital coupled-line is designed, simulated and measured at 5/5.8 GHz and applied to WLAN system. All the filters herein will be optimized using CST studio, an electromagnetic (EM) simulator.

2. ANALYSIS OF ROTATIONALLY SYMMETRICAL STRUCTURE BANDPASS FILTER

The initial filter design stems from a simple transmission line model as shown in Fig. 1(a). The filter model is symmetrical about the center of the vertical plane (A-A' plane). The signal from the input port, Port 1 or 2 is divided into two portions when passing through this two-path filter. The divided signals are then merged at the output port, Port 2 or 1. The impedance of the two models Z is chosen as $70\,\Omega$, which can be easily implemented. $|S_{21}|$ and $|S_{11}|$ are calculated from converting the resultant Y-matrix by adding the Y-matrix of upper and lower paths. $|S_{21}|$ and $|S_{11}|$ are plotted in Fig. 1(c) (dotted lines: $\theta_1 = 205^\circ$, $\theta_2 = 132^\circ$, $\theta_v = 15^\circ$), and the horizontal axis θ is a normalized frequency which can be defined as $90^\circ * f/f_0$, where f_0 is the center frequency of the passband. Since the equivalent electrical lengths for the upper and lower paths are different, signal interference occurs when these two signals are combined at the output port [19]. This signal-interference technique is expected to generate the transmission zeros in

the lower and upper stopbands, hence forming the stopbands as shown in Fig. 1(c) (dotted lines). However, this model suffers from unwanted resonance modes, at f_{m1} and f_{m2}. Fig. 1(c) shows the calculated $|S_{21}|$ and $|S_{11}|$ of Fig. 1(b) (solid line: $\theta_3 = 140°$, $\theta_4 = 75°$, $\theta_8 = 50°$, $\theta_v = 15°$). It is found that the unwanted resonance modes f_{m1} and f_{m2} are removed, whereas the passband with better than 17 dB return loss remains unchanged. The two transmission line models as shown in Fig. 1 attain good passbands at the electrical length of around 90°. The higher order modes f_{m1} and f_{m2} have been removed by adding the open-circuited stubs as shown in Fig. 1(b). However, the rejection of the out-of-bands of these two filters is poor.

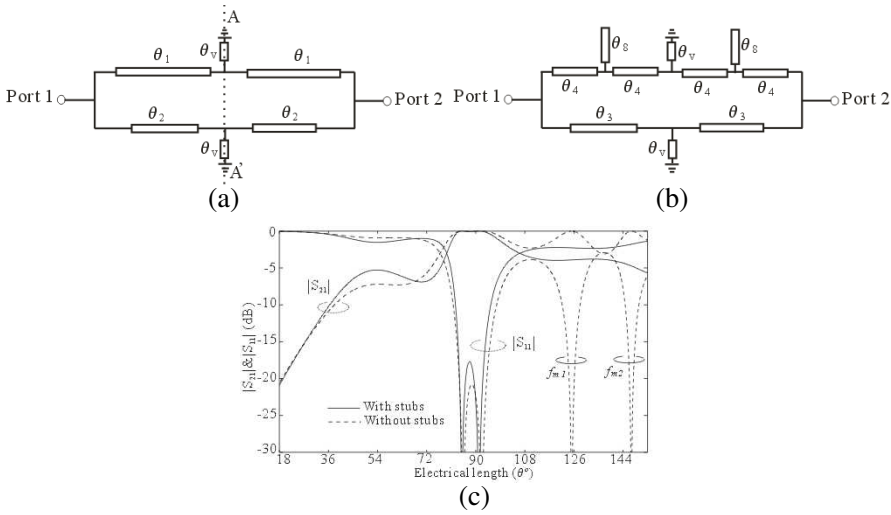

Figure 1. (a) Transmission line model of vertically symmetric filter. (b) Transmission line model of vertically symmetric filter with open-circuited stubs. (c) Calculated $|S_{21}|$ and $|S_{11}|$ of the two filter models.

The two transmission line models as shown in Fig. 1(a) and Fig. 1(b) attain good passbands at the electrical length θ of around 90° as shown in Fig. 1(c). The higher order modes f_{m1} and f_{m2} have been removed by adding the open-circuited stubs as shown in Fig. 1(b). However, the rejection of the out-of-bands of these two filters is still poor. Thus, the transmission line model as shown in Fig. 2(a) is proposed. Instead of using the vertically symmetrical structure as shown in Fig. 1, the two short-circuited stubs are offset from the center of vertical plane (plane A-A'). Thus, a rotationally symmetric structure is formed as shown in Fig. 2(a). The $|S_{21}|$ and $|S_{11}|$ are

plotted in Fig. 2(b) (solid lines: $\theta_5 = 200°$, $\theta_6 = 140°$, $\theta_v = 15°$). The transmission zeros can be easily derived from the circuit model. The Y_{12} of this model is derived as

$$Y_{12} = \frac{2j}{Z\sin(\theta_5 + \theta_6) + Z^2 \sin\theta_5 \cos\theta_6/(Z_v \tan\theta_v)} \tag{1}$$

The results from (1) are also plotted in Fig. 2(b) in a long dotted line. The transmission zeros are calculated using the intersection points of (1) and $Y_{12} = 0$ in the short dotted line. As observed from Fig. 2(b), three transmission zeros at f_{z1}, f_{z2} and f_{z3} appear at the intersection points. Notably, the rejection skirt is dramatically sharpened with the zeros at f_{z1} and f_{z2}.

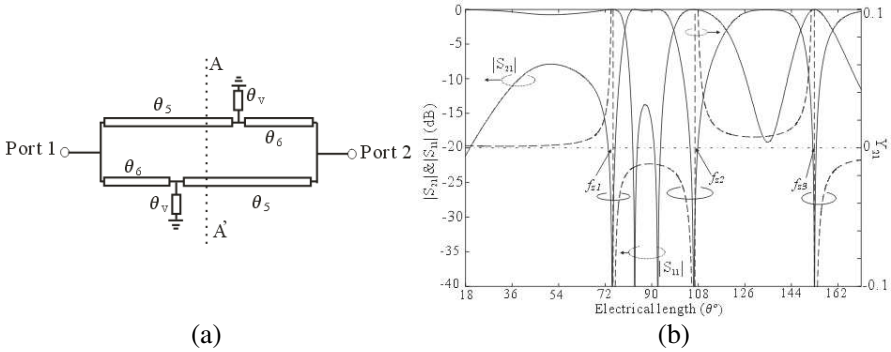

Figure 2. (a) Transmission line model of rotationally symmetric filter. (b) Calculated $|S_{21}|$, $|S_{11}|$ and Y_{21} of the filter model.

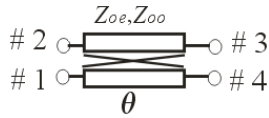

Figure 3. Transmission line model of coupled-line.

The aforementioned transmission line models are realized using microstrip-line circuits in this section. However, in the circuit implementation, a compact circuit is preferred. This leads to the transmission lines in the upper and lower sections close to each other during circuit implementation, and coupling effects should be taken into account using the coupled-line model as shown in Fig. 3.

The Z-matrix elements of the transmission line are listed

below [20]:

$$z_{11} = z_{22} = z_{33} = z_{44} = -j/2(z_{oe} + z_{oo})\cot(\theta) \quad (2a)$$

$$z_{12} = z_{21} = z_{34} = z_{43} = -j/2(z_{oe} - z_{oo})\cot(\theta) \quad (2b)$$

$$z_{13} = z_{31} = z_{24} = z_{42} = -j/2(z_{oe} - z_{oo})\csc(\theta) \quad (2c)$$

$$z_{14} = z_{41} = z_{23} = z_{32} = -j/2(z_{oe} + z_{oo})\csc(\theta) \quad (2d)$$

For instance, the model as shown in Fig. 2(a) should be reconstructed as shown in Fig. 4(a). The circuit can be divided into three parts, namely $\mathcal{Z}^a$, $\mathcal{Z}^b$ and $\mathcal{Z}^a$.

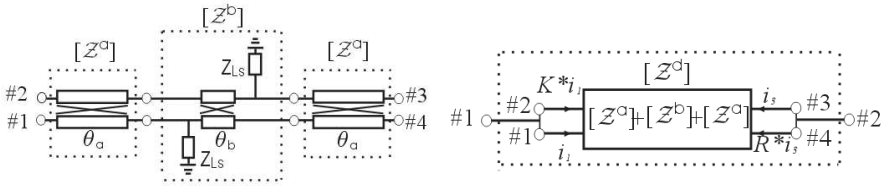

Figure 4. (a) Transmission line model of rotationally symmetric filter. (b) The equivalent network of the rotationally structure.

The $\mathcal{Z}^a$ part can be seen as simple transmission lines. The $\mathcal{Z}^b$ part can be described as two short-circuit stubs on simple transmission lines. The $\mathcal{Z}^b$-matrix of the structure in terms of coupled-line Z-matrix elements shown in Fig. 4(a) is given below:

$$Z^b_{11} = Z^b_{33} = Z_{Ls}\frac{z_{11}(Z_{Ls} - z_{11}) + z^2_{13}}{Z^2_{Ls} - z^2_{11} + z^2_{13}} \quad (3a)$$

$$Z^b_{12} = Z^b_{34} = Z_{Ls}\frac{z_{13}z_{14} - z_{11}z_{12} + z_{12}Z_{Ls}}{(Z_{Ls} - z_{11})^2 - z^2_{13}} \quad (3b)$$

$$Z^b_{13} = Z^b_{31} = Z_{Ls}\frac{z_{13}(Z_{Ls} - z_{11}) + z_{11}z_{13}}{Z^2_{Ls} - z^2_{11} + z^2_{13}} \quad (3c)$$

$$Z^b_{14} = Z^b_{32} = Z_{Ls}\frac{z_{12}z_{13} - z_{11}z_{14} + z_{14}Z_{Ls}}{(Z_{Ls} - z_{11})^2 - z^2_{13}} \quad (3d)$$

$$Z^b_{21} = Z^b_{43} = Z_{Ls}\frac{z_{12}(Z_{Ls} - z_{11}) + z_{13}z_{14}}{Z^2_{Ls} - z^2_{11} + z^2_{13}} \quad (3e)$$

$$Z^b_{22} = Z^b_{44} = z_{22} + \frac{2z_{12}z_{13}z_{14} + \left(z^2_{12} + z^2_{14}\right)(Z_{Ls} - z_{11})}{(Z_{Ls} - z_{11})^2 - z^2_{13}} \quad (3f)$$

$$Z_{23}^b = Z_{41}^b = Z_{Ls}\frac{z_{14}(Z_{Ls}-z_{11})+z_{12}z_{13}}{Z_{Ls}^2-z_{11}^2+z_{13}^2} \tag{3g}$$

$$Z_{24}^b = Z_{42}^b = z_{24}+\frac{z_{13}\left(z_{12}^2+z_{14}^2\right)+2z_{12}z_{14}\left(Z_{Ls}-z_{11}\right)}{\left(Z_{Ls}-z_{11}\right)^2-z_{13}^2} \tag{3h}$$

where, Z_{Ls} is modeling the loading effects of vias.

Figure 4(b) shows the equivalent network of the rotational structure, and $\mathcal{Z}^d$ can be easily obtained by a simple matrix addition that is $\mathcal{Z}^d = \mathcal{Z}^a(\theta_a) + \mathcal{Z}^b(\theta_b) + \mathcal{Z}^a(\theta_a)$.

By introducing two current ratios, namely K and R, to make the four-port network to two-port network, and the two-port network Z-matrix of Fig. 4(b) is obtained below by introducing K and R:

$$Z_{11} = \frac{Z_{11}^d+kZ_{11}^d}{1+k}+\frac{Z_{13}^d-Z_{14}^d}{1+k}\frac{Z_{11}^d+kZ_{12}^d-Z_{21}^d-Z_{22}^d}{Z_{23}^d-Z_{24}^d-Z_{13}^d+Z_{14}^d} \tag{4a}$$

$$Z_{12} = \frac{Z_{12}^d-Z_{11}^d}{1+R}\frac{Z_{13}^d+Z_{23}^d+R\left(Z_{14}^d+Z_{24}^d\right)}{Z_{11}^d-Z_{12}^d-Z_{21}^d+Z_{22}^d} \tag{4b}$$

$$Z_{21} = \frac{Z_{31}^d+kZ_{32}^d}{1+k}+\frac{Z_{33}^d-Z_{34}^d}{1+k}\frac{Z_{11}^d+kZ_{12}^d-Z_{21}^d-kZ_{22}^d}{Z_{23}^d-Z_{24}^d-Z_{13}^d+Z_{14}^d} \tag{4c}$$

$$Z_{22} = \frac{Z_{32}^d-Z_{31}^d}{1+R}\frac{Z_{13}^d+Z_{23}^d+R\left(Z_{14}^d+Z_{24}^d\right)}{Z_{11}^d-Z_{12}^d-Z_{21}^d+Z_{22}^d}+\frac{Z_{33}^d+RZ_{34}^d}{1+R} \tag{4d}$$

3. DESIGN OF DIPLEXER WITH ROTATIONALLY SYMMETRIC STRUCTURE

A diplexer with rotationally symmetric structure is proposed, and the layout is shown in Fig. 5(a) with marked dimensions (all in millimeters). The equivalent transmission line model is shown in Fig. 5(b), which consists of a T-junction at port 1 which divides the two desired operation frequencies into two different paths. The transmission lines connecting the filter and the input/output port are selected to satisfy the fabrication and measurement requirement. The mismatch caused by the connection lines are compensated during the filter design. The simulated insertion losses of port 2 (S_{12}) and port 3 (S_{13}) which operate at 2.4 and 2.73 GHz are 1.217 and 0.930 dB, respectively, and the return losses of port 2 (S_{22}) and port 3 (S_{33}) are better than 17 dB at 2.4 GHz and 15 dB at 2.73 GHz. The isolation of two output ports (port 2 and port 3) is better than 23 dB as shown in Fig. 5(c).

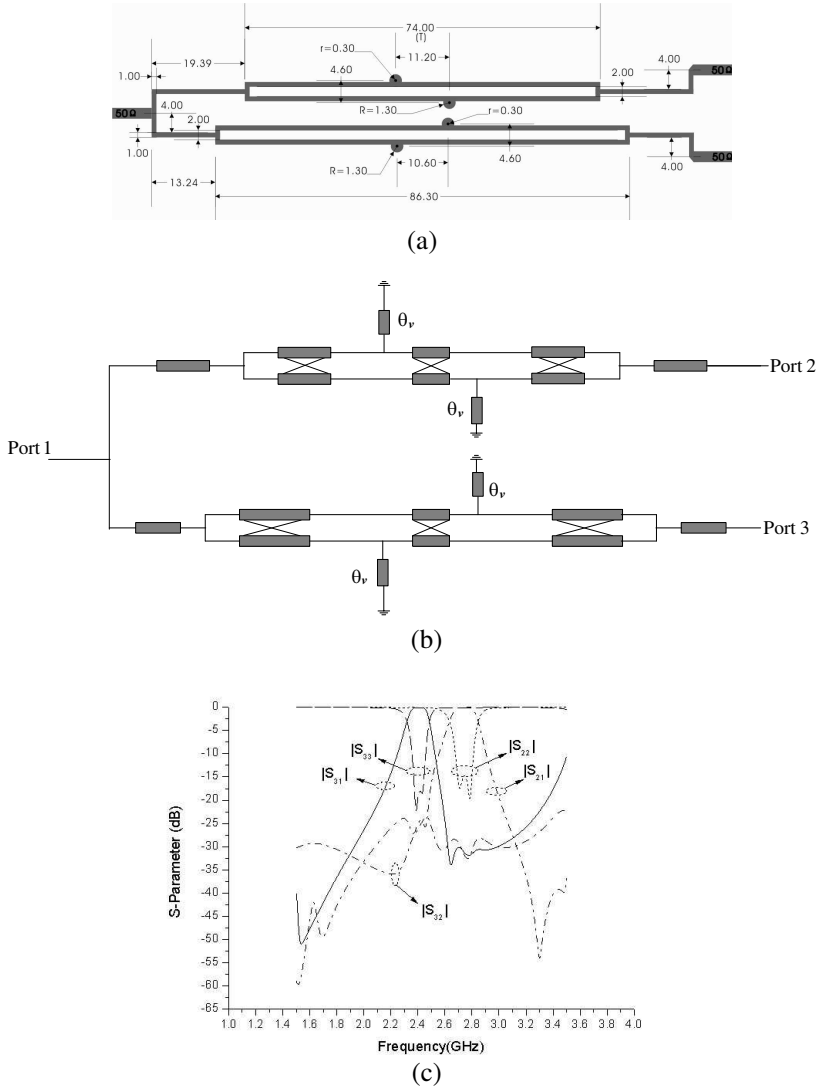

Figure 5. (a) Circuit layout with marked dimensions of proposed diplexer. (b) Equivalent circuit model of proposed diplexer. (c) Simulated S-parameters of proposed diplexer.

Moreover, the higher passband can be controlled simply by appropriately selecting the length of the rotationally symmetric structure, which can be describe as the T shown in Fig. 5(a), and the T value is one wavelength at center frequency of 2.7 GHz. As

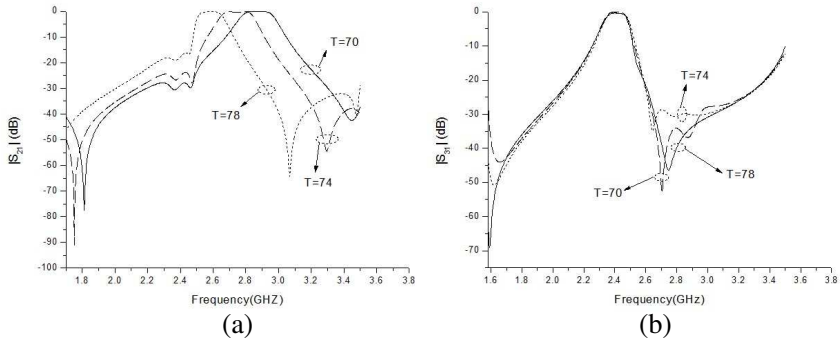

Figure 6. (a) Simulation $|S_{21}|$ results of varied values of T. (b) Simulation $|S_{31}|$ results of varied values of T.

can be observed in Fig. 6(a) and Fig. 6(b), the lower frequency passband remains unchanged while the higher passband shifts to higher frequency as variable T is decreased from 78 mm to 70 mm. This shows an attractive property that the higher or lower frequency band can be controlled individually.

4. ROTATIONALLY SYMMETRIC STRUCTURE WITH INTERDIGITAL COUPLED LINES

The interdigital coupled-lines are proposed to improve the out-of-band performance of the proposed rotationally symmetric diplexer. Fig. 7(a) shows the layout with the detailed dimensions of the proposed diplexer designed at 5 GHz/5.8 GHz for WLAN system (all in millimeters). The simulated results are shown in Fig. 7(c). Obviously, the filter with interdigital coupled-lines has achieved a sharper roll-off rejection skirt than the filter shown in Fig. 5(c) because of the two transmission zeros of the interdigital coupled-lines filter closer to the cut-off edges of the passband. An equivalent circuit network of one passband of the proposed rotationally symmetric structure is given in Fig. 7(b). As can be observed in Fig. 7(b), the interdigital sections are modeled as J-inverters which produce a higher order bandpass filter. It is well known that the higher a filter's order is, the sharper the selectivity of a filter is. Thus, the rejection skirt in Fig. 7(c) is sharper than that in Fig. 5(c). The simulated insertion losses of port 2 (S_{12}) and port 3 (S_{13}) which operate at 5 and 5.8 GHz are 0.95 dB and 1.03 dB, respectively, and the return losses of port 2 (S_{22}) and port 3 (S_{33}) are better than 11 dB at 5 GHz and 13 dB at 5.8 GHz. The isolation of

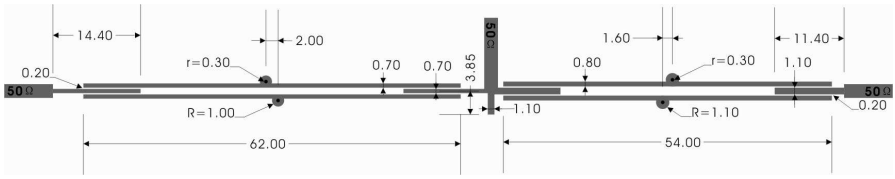

(a)

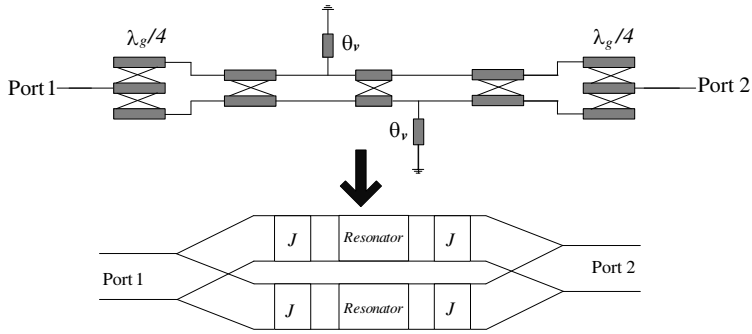

(b)

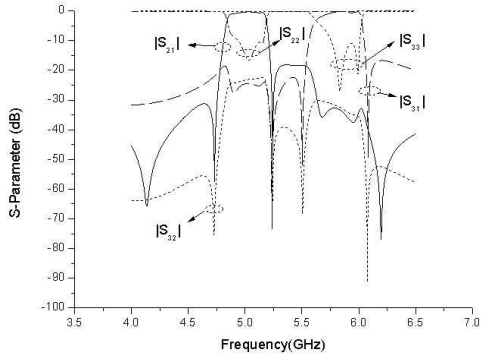

(c)

Figure 7. (a) Circuit layout of the designed diplexer in the original structure with intedigital structure. (b) Equivalent circuit network of one of passband of proposed interdigital filter structure. (c) Simulated S-parameters of proposed diplexer in original structure.

two output ports (port 2 and port 3) is better than 24 dB as shown in Fig. 7(c).

In order to reduce the size and keep the excellent in- and out-of-band performance, an improved structure based on the original one is proposed, which is shown in Fig. 8(a) (all in millimeters).

The transmission line model of the rotationally symmetric structure with interdigital coupled line is shown in Fig. 8(b), and can be seen as divided into the upper and lower resonators. The input power is coupled to the two resonators through the two sections of one-quarter guided wavelength ($\lambda_g/4$, λ_g at 5 GHz and 5.8 GHz) interdigital coupled-lines sections. The modeling of the interdigital coupled-lines

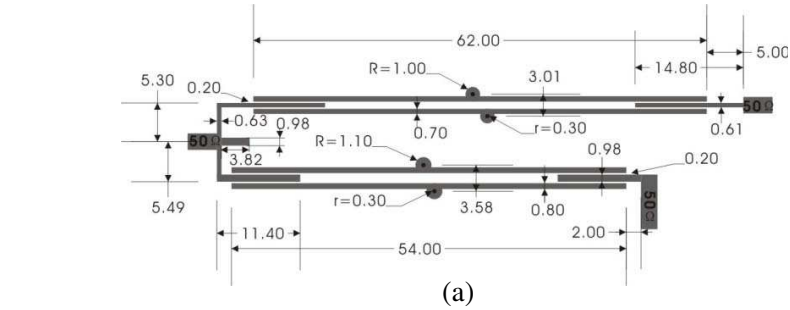

(a)

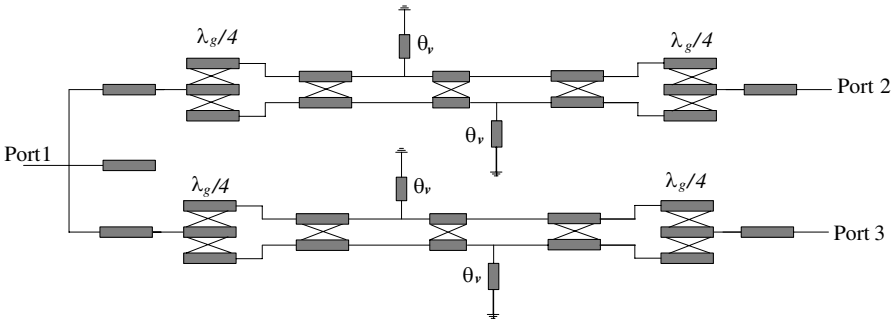

(b)

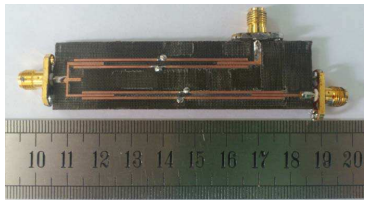

(c)

Figure 8. Circuit layout of the designed diplexer of the improved structure. (a) Schematic with marked dimensions. (b) Equivalent circuit model of proposed diplexer with inter-digital coupled line. (c) Photograph of fabricated diplexer.

involves c-mode and π-mode due to the asymmetrical coupling [21, 22]. As known, it is difficult to convert both the c- and π-modes to physical dimensions in filter design. Thus, both the c- and π-modes are simplified into the even- and odd-modes [23]. Under the premise of ensuring isolation between the two passbands, the improved structure is designed with a compact size. In order to verify the proposed structure, the diplexer with rotationally symmetric structure and interdigital coupled-lines is fabricated and measured, and the substrate used herein has a dielectric constant of 2.55 and thickness of 0.8 mm for designing the proposed diplexer. Fig. 8(c) shows a photograph of fabricated circuit.

Figure 9 shows the simulated and measured S-parameter results of the proposed diplexer with interdigital coupled-lines. The measured insertion losses of port 2 (S_{12}) and port 3 (S_{13}) which operate at 5

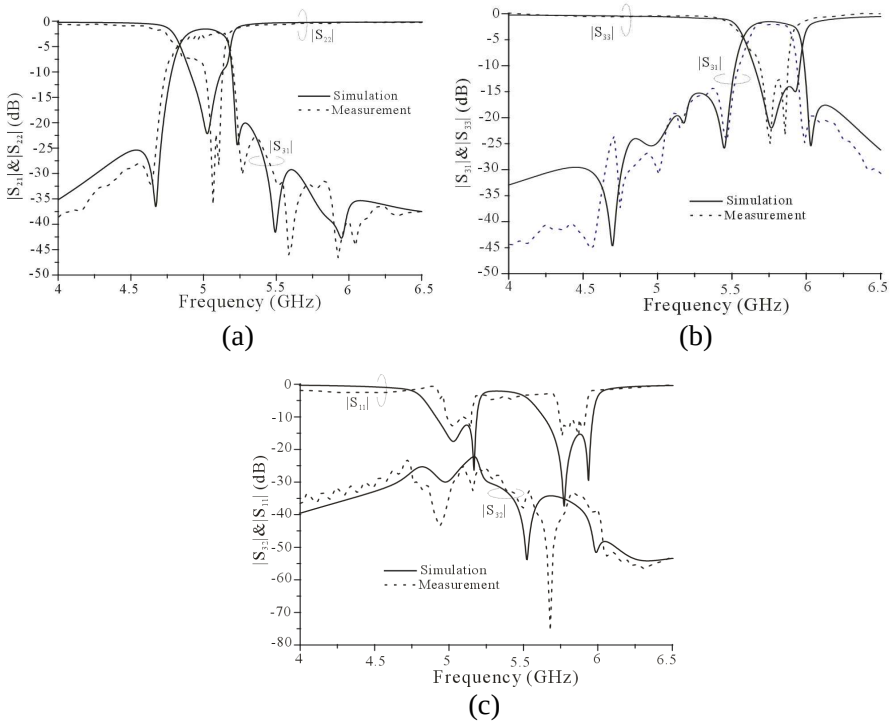

Figure 9. Simulated and measured results of S-parameter. (a) $|S_{21}|$, $|S_{22}|$ of the proposed structure with interdigital coupled-lines. (b) $|S_{31}|$ and $|S_{33}|$ of the proposed structure with interdigital coupled-lines. (c) $|S_{11}|$ and $|S_{32}|$ of the proposed structure interdigital coupled-lines.

and 5.8 GHz are 1.524 and 1.526 dB, respectively. Port 1's return loss (S_{11}) is better than 11/12 dB, and the return losses of port 2 (S_{22}) and port 3 (S_{33}) are better than 22 dB at 5 GHz and 14 dB at 5.8 GHz. The isolation of two output ports (port 2 and port3) is better than 22 dB as shown in Fig. 9(c). Moreover, pairs of transmission zeros are allocated at the two sides of the passband clearly. A good filter performance and miniaturization of the proposed diplexer are achieved by using the rotational structure with interdigital coupled-lines.

5. CONCLUSION

A diplexer with rotationally symmetric structure is proposed and studied in this paper. We propose two types of diplexers with rotationally symmetric structure. The first one is designed at 2.4 GHz/2.73 GHz, and the second one at 5/5.6 GHz for WLAN system. For verification, one prototype based on rotationally symmetric structure with interdigital coupled lines structure is fabricated and measured. Good agreement between the simulated and measured results has been observed, which demonstrates that the proposed circuit fulfills predicted results, good isolation between two output ports with more than 22 dB and good impedance matching and insertion loss of 1.524/1.524 dB at 5/5.8 GHz. Port 1's return loss (S_{11}) is better than 11/12 dB, and the return losses of port 2 (S_{22}) and port 3 (S_{33}) are better than 22 dB at 5 GHz and 14 dB at 5.8 GHz. The microstrip diplexer of the rotationally symmetric structure is an attractive design for further development and applications in modern communication systems, which is simple and easy to be integrated.

ACKNOWLEDGMENT

This work is supported by the National Natural Science Foundation of China (61101017) and the State Key Laboratory of Millimeter Waves (K201327), Southeast of University.

REFERENCES

1. Sze, J.-Y., T.-H. Hu, and T.-J. Chen, "Compact dual-band annular-ring slot antenna with meandered grounded strip," *Progress In Electromagnetics Research*, Vol. 95, 299–308, 2009.
2. Shi, L., H.-J. Sun, W.-W. Dong, and X. Lv, "A dual-band multi-function carborne hybrid antenna for satellite communication relay system," *Progress In Electromagnetics Research*, Vol. 95, 329–340, 2009.

3. Behera, S. and K. J. Vinoy, "Microstrip square ring antenna for dual-band operation," *Progress In Electromagnetics Research*, Vol. 93, 41–56, 2009.
4. Tilanthe, P., P. C. Sharma, and T. K. Bandopadhyay, "A monopole microstrip antenna with enhanced dual band rejection for UWB application," *Progress In Electromagnetics Research B*, Vol. 38, 315–331, 2012.
5. Wang, X.-H., B.-Z. Wang, and K. J. Chen, "Compact broadband dual-band bandpass filters using slotted ground structures," *Progress In Electromagnetics Research*, Vol. 82, 151–166, 2008.
6. Chen, Z.-X., X.-W. Dai, and C.-H. Liang, "Novel dual-mode dual-band bandpass filter using double square-loop structure," *Progress In Electromagnetics Research*, Vol. 77, 409–416, 2007.
7. Patin, J. M., N. R. Labadie, and S. K. Sharma, "Investigations on an H-fractal wideband microstrip filter with multi-passbands and a tuned notch band," *Progress In Electromagnetics Research B*, Vol. 22, 285–303, 2010.
8. Chen, M., Y.-C. Lin, and M.-H. Ho, "Quasi-lumped design of bandpass filter using combined CPW and microstrip," *Progress In Electromagnetics Research Letters*, Vol. 9, 59–66, 2009.
9. Wu, Y., Y. Liu, and S. Li, "A compact pi-structure dual band transformer," *Progress In Electromagnetics Research*, Vol. 88, 121–134, 2008.
10. Castaldi, G., V. Fiumara, and I. Gallina, "An exact synthesis method for dual-band chebyshev impedance transformers," *Progress In Electromagnetics Research*, Vol. 88, 305–319, 2008.
11. Strassner, B. and K. Chang, "Wide-band low-loss high isolation microstrip periodic-stub diplexer for multiple-frequency applications," *IEEE Trans. Microw. Theory Tech.*, Vol. 49, No. 10, 1818–1820, 2001.
12. Wang, R., J. Xu, M.-Y. Wang, and Y.-L. Dong, "Synthesis of microwave resonator diplexers using linear frequency transformation and optimization," *Progress In Electromagnetics Research*, Vol. 124, 441–455, 2012.
13. Chen, C.-F., T.-Y. Huang, C.-P. Chou, and R.-B. Wu, "Microstrip diplexers design with common resonator sections for compact size, but high isolation," *IEEE Trans. Microw. Theory Tech.*, Vol. 54, No. 5, May 2006.
14. An, J., G.-M. Wang, C.-X. Zhang, and P. Zhang, "Diplexer using composite right-/left-handed transmission line," *Electronics Letters,* Vol. 44, No. 11, May 22, 2008.

15. Yang, R.-Y., C.-M. Hsiung, C.-Y. Hung, and C.-C. Lin, "Design of a high band isolation diplexer for GPS and WLAN system using modified stepped-impedance resonators," *Progress In Electromagnetics Research*, Vol. 107, 101–114, 2010.
16. Huang, C.-Y., M.-H. Weng, and C.-S. Ye, "A high band isolation and wide stopband diplexer using dual-mode stepped-impedance resonators," *Progress In Electromagnetics Research*, Vol. 100, 299–308, 2010.
17. Shi, J., J.-X. Chen, and Z.-H. Bao, "Diplexers based on microstrip line resonators with loaded elements," *Progress In Electromagnetics Research*, Vol. 115, 423–439, 2011.
18. Wong, S. W., K. Wang, Z.-N. Chen, and Q.-X. Chu, "Rotationally symmetric coupled-lines bandpass filter with two transmission zeros," *Progress In Electromagnetics Research*, Vol. 135, 641–656, 2013.
19. Gomez-Garcia, R. and J. I. Alonso, "Design of sharp-rejection and low-loss wide-band planar filters using signal-interference techniques," *IEEE Microwave Wireless Compon. Lett.,* Vol. 15, No. 8, 530–532, Aug. 2005.
20. Zysman, G. I. and A. K. Johnson, "Coupled transmission line networks in an inhomogeneous dielectric medium," *IEEE Trans. Microw. Theory Tech.*, Vol. 17, No. 10, 753–759, Oct. 1969.
21. Schwindt, R. and C. Nguyen, "Spectral domain analysis of three symmetric coupled lines and application to a new bandpass filter," *IEEE Trans. Microw. Theory Tech.*, Vol. 42, No. 7, 1183–1189, Jul. 1994.
22. Tripathi, V. K., "On the analysis of symmetrical three-line microstrip circuits," *IEEE Trans. Microw. Theory Tech.*, Vol. 25, No. 9, 726–729, Sept. 1977.
23. Hong, J. S. and M. J. Lancaster, *Microstrip Filters for RF/Microwave Applications*, Wiley, New York, 2001